Iranian Journal of Hydrogen & Fuel Cell 4(2017) 249-263

Iranian Journal of Hydrogen & Fuel Cell

IJHFC

Journal homepage://ijhfc.irost.ir

Numerical study on the performance prediction of a proton exchange membrane (PEM) fuel cell

Puriya Mohamad Gholy Nejad, Ali Reza Solaimany Nazar*, Zohreh Rahimi-Ahar, Zohreh Karami

Department of Chemical Engineering, University of Isfahan, Isfahan, Iran

Article Information

Article History:

Received:
14 Nov 2017
Received in revised form:
08 Jan 2018
Accepted:
10 Jan 2018

Keywords

PEM fuel cell
Catalyst layer
Gas diffusion layer
Power density
Performance

Abstract

An electrochemical analysis on a single channel PEM fuel cell was carried out by Computational Fuel Cell Dynamics (CFCD). The objective was to assess the latest developments regarding the effects of change in the current collector materials, porosity of electrodes and gas diffusion layer on the fuel cell power density. Graphite, as the most applicable current collector material, was applied followed by Aluminum and Titanium. It was found that titanium enhances the performance of the fuel cell as compared to the graphite and aluminum. Other results obtained were: the total porosity of the electrodes' layers does not have a significant effect on power density. An higher porosity of gas diffusion layer at voltages higher than 0.5 is favorable in gas diffusion, which leads to better performance. A numerical model, based on the assessment of basic best practice guidelines for CFCD, was developed that led to reasonably good agreement with the experimental results.

1. Introduction

Due to increasing pollutant emissions caused by fossil fuels, studies on renewable energies have gained importance. The fuel cell is an electrochemical device that allows the effective exchange of chemical energy stored in a fuel cell together with an oxidant to produce electrical energy. Fuel cells are generally

*Corresponding Author's Fax: +983137934031
E-mail address: asolaimany@eng.ui.ac.ir

doi: 10.22104/ijhfc.2018.2587.1159

divided into five important types differentiated from one another by their electrolyte: Phosphoric Acid Fuel Cell (PAFC), Proton Exchange Membrane Fuel Cell (PEMFC), Solid Oxide Fuel Cell (SOFC), Alkaline Fuel Cell (AFC) and Molten Carbonate Fuel Cell (MCFC). Several technological arrangements have been studied according to different electrolytes and operating temperatures [1]. Of the high temperature fuel cells SOFCs and MCFCs and PEMFCs of the low temperature fuel cells have been widely focused on by researchers. PEMFCs are common in fuel cells studies because of their low operating temperature and therefore low emission, high efficiency and power density. The efficiency of these fuel cells is around 43- 58% [2, 3]. They are used mainly in transferring applications with low polluting potential.

1.1. Fuel cell operation

In order to provide a sizable reaction areawhich will produce higher electricity, the fuel cells are usually thin with a planer structure. One side of this planer structure is supplied with fuel and the other with oxidant. The reactant delivery, electrochemical reaction, product removal from fuel cell, ionic conduction through the electrolyte and electronic conduction through the external circuit lead to the production of electricity in a fuel cell. A typical PEMFC has three parts: a proton exchange membrane, a cathode and an anode both of which are made up of three regions consisting of: the catalyst layer (CL), the gas channel and the gas diffusion layer (GDL). Polymer membranes have special capabilities which are impermeability to gases and permeability to proton. The membrane is coated with thin layers of catalyst and is put between two bipolar plates (BPs) which supply fuel and oxidant for the chemical reaction. The electrodes are made of graphite, titanium, stainless steel and other related materials. Each one of these materials has their advantages and disadvantages in terms of corrosion, conductivity, mechanical properties, weight and cost. The BP has five distinct functions: distributing the fuel and oxidants in the cell, separating cells in the stack, facilitating water and controlling heat in the cell, and transmitting currents from the cell [4]. The catalyst materials are usually platinum, gold and palladium [5]. Different researchers [6, 7] have concentrated on various structures to protect metallic BPs based on a thin and inert electrically conductive coating layer. The parameters for choosing the BP and the catalyst materials are: light weight, low coating cost, high efficiency, durability and low contact resistance. They expressed that the greatest level of success in achieving an appropriate coating material is through consuming gold and palladium [8].

An electrochemical reaction occurs at the catalyst surface. Hydrogen (H_2) is fed to the fuel cell where it splits into protons and electrons. The protons and the electrons pass through the membrane and the collectors, respectively, to produce electricity. A sketch of a typical PEMFC is shown in Fig. 1.

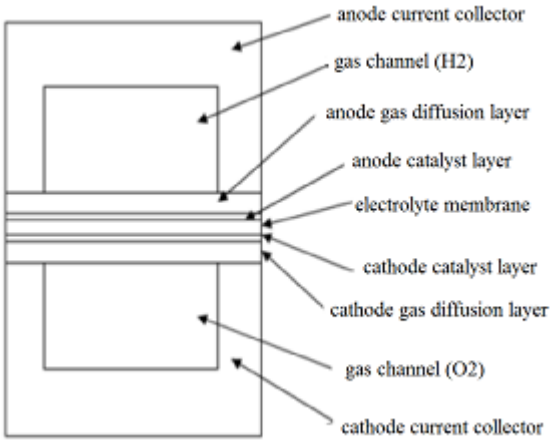

Fig. 1. Sketch of a typical PEMFC [9].

One of the effective manners to enhance anode and cathode catalyst utilization is to increase the CL porosity in order to exposed catalyst clusters to the maximum extent of gas reactants and to increase the reaction sites allowing easy water flow out of the CL, which will result in a low diffusion resistance. The CLs should be of the same catalyst otherwise the measured data will be the average of the two different CLs.

In order to improve reactant gas distribution in the PEMFC channel, where pin fins are inserted in channel, Obayopo et al. [10] ran an assessment on the flow field and reactant gas distribution in this channel. They concluded that channel friction and hence pressure drop are reduced by an increase in GDL porosity. Another study on GDL porosity was conducted by Wang et al. [11], they remarked that the cathode GDL and CL porosities have a major effect on cell performance, while the anode GDL and CL porosities have an insignificant effect. They deduced that optimization of GDL and CL cathode parameters is more significant in enhancing the fuel cell performance than that of anode GDL and CL.

The physics of the fuel cells are complex with many processes occurring in them. Since the setup for fuel cell experiments is expensive and due to improvements in computer calculation speed, computational fluid dynamics (CFD) modeling can be an effective tool in greater understanding of the complex hydrodynamics of fuel cells. The CFD model should be coupled with an electrochemical model for predicting the species transfer and the electrochemical reactions. Several CFD numerical models of fuel cells have been developed by researchers [12, 13], who have concentrated on the specific parts of the PEMFC like the BP, CL, GDL and membrane. Taymaz et al. [14] developed a CFD simulated PEMFC of single channel model. The results indicate that the coefficients of diffusion and permeability depend on the porosity of the GDL, which was reduced by the compression of the assembly pressure. The influence and optimum values of the parameters, including porosity, cathode/ anode permeability, the thickness of the GDL, and the inlet gas stoichiometric ratio, on the performance of fuel cells were identified by Zhang et al. [15]. They found that an optimized oxygen mole fraction and the current density distribution provide valuable information for superior design of a fuel cell.

3D modeling of a SOFC was investigated by Ebrahimi et al. [16] to attain the optimized cell operation. Radiation heat transfers between the channel wall and the fluid as well as the cell and ambient outside was employed. Cathode layer thickness optimizing was conducted based on minimizing the ohmic drop. Utilizing this optimization simulation, the maximum current density was obtained. 3-D geometries for flow fields of the cathode and anode was developed by Farzin et al. [17]. on the aim was to study the comparative impact of increasing the multiplicity of the anode-cathode channel surface contact on the efficiency of the electrochemical reaction. The same membrane electrode assembly active area was considered. In the proposed models, the anode channel includes two, three and four cathodes in comparison with the conventional model which consists of a one to one connection. The results revealed that increasing the multiplicity of the anode-cathode leads to an increase in the current and power density. This was due to the improved opportunity of reactants penetration and less concentration losses. Other advantages of the proposed models were a considerable reduction of mono-cell volume size and cost.

Rostami et al. [18] studied the serpentine flow channel with different bend sizes in a PEMFC.

Ignoring drying in the anode and flooding in cathode, a single-phase model was developed. They changed the bend sizes from 0.8 mm to 1.2 mm to reduce the mass transport loss at a minimum pressure drop. It was concluded that an increase in bend size leads to increases in reaction area, thickness of boundary layer and temperature gradient. More uniform distribution of electrolytes over the electrode occurred, which increased the power density of the fuel cell by 1.78%. Moreover, serpentine flow channels with 1.2 mm bend size prevented secondary flows; hence, reducing the pressure drop by 90.6%.

The performance of a PEMFC was mathematically studied by Vasilyev et al. [19]. A model was developed based on the bond graph technique in Modelica language. The proposed method was introduced as a popular method within the fuel cell modeling community due to its versatility in the application area. Other features of the proposed model were its hierarchical structure and adaptation of multi-bonds for the analysis of multicomponent mixtures. The mass flow controllers, bipolar plates, cooling channels and membrane electrode assembly were created. This enabled a streamlined graphical portrayal of the process and was beneficial for bond-graphic implementation of such phenomena. Jithin et al. [20] studied heat and mass transport with reaction in a PEMFC using the lattice Boltzmann method. They considered the heat generation due to oxygen reduction and its effects on heat transport and reaction. The effects of different cell operating voltages, temperatures and flow rates as well as porosity, permeability and effective porous media diffusion coefficient on fuel cell performance were studied. They concluded that output power density is limited by the mass transport rate. An increase in operating temperature led to an increase in current density; hence, an increase in the rate of heat generation. Porosity and permeability of the gas diffusion layer had no significant effect on the performance in the studied ranges; however, higher permeability enhanced the thermal gradients in the porous layer. Due to higher convection and better transport of species by increasing the flow rates, a significant increase in the maximum current density was concluded. The fuel utilization was enhanced at high diffusion rates in the porous media.

1.2. Research Objectives

The literature review indicates the lack of sufficient studies in fuel cells that are subject to different collectors' material, anode/cathode CL porosity and GDL porosity. The objectives are summarized as follows:

I. Create a single channel PEMFC numerical model with nine zones consisting of two BPs, two gas flow channels, two GDLs, two CLs and a membrane.

II. Simulate the electrochemical phenomena and obtain the fuel cell performance, and validate the model against available published experimental data.

III. Run an assessment on voltage changing and its effect on power density in order to evaluate the efficient voltage.

IV. Change the collectors' material and carry out the related analysis in order to fabricate a high performance fuel cell.

V. Investigate the effect of the anode/cathode CL and GDL porosities on power density, hence, evaluate the proper porosity.

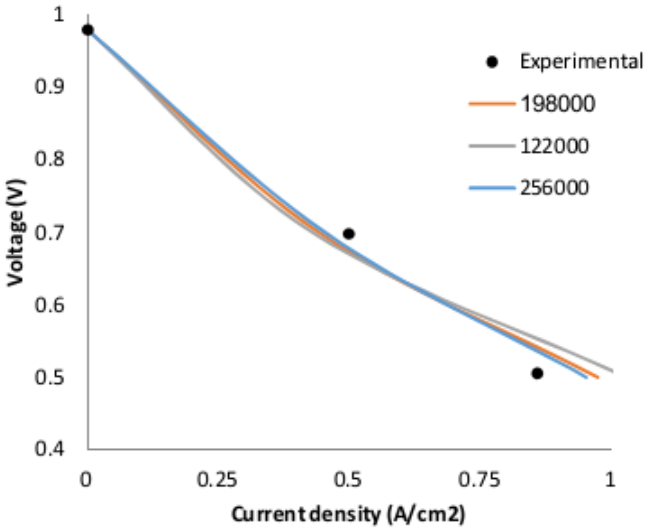

Fig. 2. Mesh independence analysis of a PEMFC.

2. Numerical solution

The modeling here is carried out in order to predict the influence of changes in: voltage, material of collectors, and porosities of CL and GDL on power density.

2.1. Geometry and Grid independency

The modeling was carried out by developing a PEMFC, Fig. 1 [9]. The different parts of the fuel cell were assembled in three stages using appropriate constrains to form the complete PEMFC assembly. In the first stage, the geometry of a commercial 50 cm2 cell was formed. In the second stage, the mesh from the geometry was developed. In order to consider the inflation near the walls, fine meshes near the walls were created. In order to solve the equations associated with a fuel cell simulation, the geometry was divided into computational cells using a hexahedral mesh. A mesh independence analysis was carried out to assess mesh independency. For this purpose, 122000, 198000 and 256000 cells were tested. As no further significant change was found for finer cells, the appropriate number of cells was determined and the final mesh of 198000 cells was selected (see Fig. 2). The optimized computational mesh with 198000 cells is illustrated in Fig. 3. The third stage, adoption of boundary conditions according to physical and operating parameters of PEMFC for solving the above mentioned reaction kinetics by finite volume method. The dimensions of the model are tabulated in Table 1.

2.2. Solver

The standard physical conservation equations [mass continuity, momentum, chemical species (H_2O, H_2

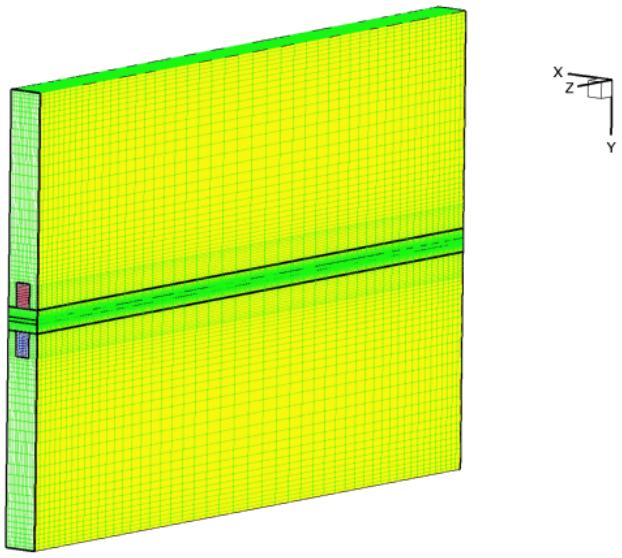

Fig. 3. The discretized 3D computational domain of a PEMFC.

Table 1. Dimensions of the simulated PEMFC

Dimension	Value (mm)
Gas channel length	30
Gas channel width	0.86
Gas channel height	1.1
GDL height	0.6
CL height	0.06
Membrane height	0.175
Current collector width	1.57

and O_2), solid phase potential, membrane phase potential, liquid saturation, and water content based on basic best practice guidelines for CFCD are solved [21]. The simulation is run in the 3D steady state, double precision and parallel processing, by ideal gases, laminar flow, incompressible fluid, constant thermophysical properties, porous GDL, the isotropic two CLs and the membrane [12, 13]. The SIMPLE pressure–velocity coupling algorithm, the atmospheric pressure and the second order upwind discretization scheme for momentum are applied.

2.3. Initial and boundary conditions

In this study, there exist two inlets: hydrogen and water (anode) and oxygen and water (cathode). A uniform velocity inlet boundary condition is given for both inlets. The fuel is fed into the fuel cell as a mixture of gases. The flows of H_2 and O_2 are in opposite directions. The mass flow rates at the anode and cathode are 5.599375×10^{-7} and 9.843×10^{-6} (kg/s), respectively. The outlet boundary condition is the pressure outlet. The voltages are 0.4, 0.5, 0.6, 0.7, 0.8 and 0.95 (V) were selected for their potential in solving the reaction. The species concentration on the cathode side of H_2, O_2, and H_2O are 0, 0.1785 and 0.15 (mol/m^3), respectively, and on the anode side are 0.5, 0 and 0.5 (mol/m^3), respectively. The CL porosities of anode and cathode are 0.4, 0.5 and 0.6. The GDL porosities are changed as follows: 0.7, 0.82 and 0.92. The no-slip boundary condition is imposed on the walls. Some model parameters are affected by the compression or operating conditions (e.g. GDL porosity and electric conductivity). The briefed values for the parameters are tabulated in Table 2.

Table 2. PEMFC parameters in simulation [9]

Parameter	Value (unit)
ρ_{BP}	1990 (kg/m^3)
$C_{P_{BP}}$	710 (J/kg.K)
K_{BP}	120 (W/m.K)
σ_{BP}	92600 (1/U.m)
δ_{BP} [In-situ measurement]	9.5 (mm)
BP- GDL contact resistance (parallel) [In-situ measurement]	4.56e-6 (Ω.m^2)
BP- GDL contact resistance (serpentine) [In-situ measurement]	3.52e-7 (Ω.m^2)
ρ_{GDL}	32105 (kg/m^3)
ε_{GDL}	0.82
Σ_{GDL}	280 (1/U.m)
Anode GDL viscous resistance	1.0e12 (1/m^2)
Cathode GDL viscous resistance	3.86e12 (1/ m^2)
GDL wall contact angle	110°
δ_{GDL}	420 (mm)
CL surface-to-volume ratio eq. (13)	1.25e7 (m^2/m^3)
δ_{CL} (anode)	6 (mm)
δ_{CL} (cathode)	12 (mm)
$\rho_{membrane}$	1980 (kg/m^3)
$K_{membrane}$	0.16 (W/m.K)
Membrane equivalent weight	110 (kg/kmol)
$\delta_{membrane}$	175 (mm)
Open circuit voltage [In-situ measurement]	0.98 (V)
Γ_{H_2}	8.0e-5 (m^2/s)
Γ_{O_2}	2.0e-5 (m^2/s)
Γ_{H_2O}	5.0e-5 (m^2/s)

2.4. Governing Equations

To simulate a model of a fuel cell, a full understanding of the standard physical conservation equations is of essence. The 3D fluid flow is modeled by the Navier-Stokes transfer with transfer equations as follows [9]:

$$\frac{\partial}{\partial t}\int_{V}\rho\phi dV+\oint_{A}\rho\phi V.\,dA=\oint_{A}\Gamma_{\phi}\nabla\varnothing.dA+\int_{V}S_{\phi}dV \quad (1)$$

Two potential equations are solved for the solid (j=solid) and the membrane phase (j=membrane) [9].

$$\nabla.\left(\sigma_{j}\nabla\varphi_{j}\right)+R_{j}=0 \quad (2)$$

The pressure drop in CL and GDL due to the fluid flow is characterized by adding a negative source term to the momentum equations [22] as follows:

$$S_{i}=-\left(\frac{\mu}{k}\nu_{i}+C_{2}\frac{1}{2}\rho\nu_{mag}\nu_{i}\right) \quad (3)$$

Multi-species diffusivities in GDL are calculated by considering the pore blockage according to [23]:

$$D_{i}=\epsilon^{1.5}\left(1-s\right)^{r_{s}}D_{i}^{ref}\left(\frac{p_{ref}}{p}\right)\left(\frac{T_{ref}}{T}\right)^{1.5} \quad (4)$$

The volumetric source terms are added to the energy equation and calculated through the Butler–Volmer equation as follows [9]:

$$R_{an}=i_{an}^{ref}\left(\frac{C_{H_2}}{C_{H_2}^{ref}}\right)^{\gamma^{an}}\left(e^{-\left(\alpha_{an}\frac{F}{RT}\right)\eta_{an}}-e^{-\left(\alpha_{cat}\frac{F}{RT}\right)\eta_{cat}}\right) \quad (5)$$

$$R_{cat}=i_{cat}^{ref}\left(\frac{C_{O_2}}{C_{O_2}^{ref}}\right)^{\gamma^{cat}}\left(e^{-\left(\alpha_{cat}\frac{F}{RT}\right)\eta_{cat}}-e^{-\left(\alpha_{an}\frac{F}{RT}\right)\eta_{an}}\right) \quad (6)$$

In the gas channel, GDLs and membrane, the source term is set at zero. The source rates depend on the electrochemical reaction rates for the chemical species and are considered in the electrochemical reaction as follows:

$$S_{H_2}\left(kgs^{-1}m^{-3}\right)=-\frac{M_{w},H_{2}}{2F}R_{anode} \quad (7)$$

$$S_{O_2}\left(kgs^{-1}m^{-3}\right)=-\frac{M_{w},O_{2}}{4F}R_{cathode} \quad (8)$$

$$S_{H2O}\left(kgs^{-1}m^{-3}\right)=-\frac{M_{w},H2O}{2F}R_{cathode} \quad (9)$$

The conservation equation for the H_2O saturation is presented as follows [24]:

$$\frac{\partial\left(\epsilon\rho_{1}S\right)}{\partial t}+\nabla.\left(\rho_{1}\vec{V_{1}}s\right)=r_{w} \quad (10)$$

Inside the porous zones the capillary diffusion term replaces the convective term and equation (10) changes to following equation [24]:

$$\frac{\partial\left(\epsilon\rho_{1}S\right)}{\partial t}+\frac{d}{ds}\nabla.\left(\rho_{1}\frac{Ks^{3}}{1}\frac{dp_{c}}{}\nabla s\right)=r_{w} \quad (11)$$

Equation (11) takes into account the transfer phenomena inside GDL.

Water produced due to the cathodic reaction in the PEMFCs penetrates to the anode side due to back diffusion and electro-osmosis force. Water content (λ) transfers through the membrane, as an important parameter developed by Springer et al. [25]:

$$\lambda=\left\{0.043+17.81a-39.85a^{2}+36a^{3}\right\}\quad 0\le a\le 1 \quad (12)$$

$$\lambda=\left\{14+1.4\left(a-1\right)\right\}\quad 0\le a\le 3 \quad (13)$$

where [9];

$$a=P_{v}/P_{sat}+2s \quad (14)$$

2.5. Validation

The simulation was run by considering a 3D PEMFC model. Essentially, the PEMFC model solves conservation of mass, momentum, species, and the charge in the functional layers of the fuel cell containing the BP, flow field, porous backing, CL and membrane. The polarization (voltage–current) curve is one of the important final results of CFD simulations and can be used to describe the fuel cell performance and for validation purposes [26]. The simulation results for the reference operating conditions are verified against experimental data of Iranzao et al. [27]. The obtained polarization curve is illustrated in Fig. 4, where a good agreement with

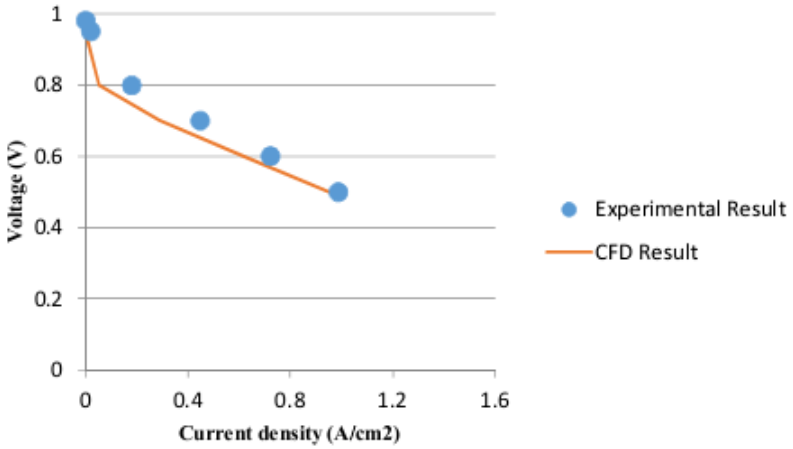

Fig. 4. Comparison of polarization curves in the simulation model and experimental study.

the experimental result is observed. Comparison between the obtained CFD results in the present study with the results obtained through experimental study indicates the maximum errors of 1.86 %.

As observed, the fuel cell performance increases with a decrease in voltage. The fuel cell output voltage influences the current density; thus, the total power production. The total power produced by the fuel cell is the product of current and voltage, P = iV. The current supplied by a fuel cell is directly proportional to the amount of the fuel consumed. Using this relationship, it can be claimed that fuel cell voltage is a measure of fuel cell efficiency.

3. Result and discussion

Utilizing the techniques described above, we determined the performance of the fuel cell by conducting tests to obtain polarization curves for each sample and then characterizing the effects of changes in the collectors' material, electrode CL and GDL porosities on the power density.

3.1. Effect of collector material on power density

Current collectors are applied to collect the generated current in the fuel cells and provide passage for the reactants. A current collector of good material in a fuel cell subject to higher electrical conductivity leads to lower electrical resistivity, hence, higher performance. The current collectors are in direct contact with the electrodes. Pressure may damage them and electrochemical reaction products (H_2O and CO_2) in the fuel cell may cause the collectors to deteriorate, therefore; choosing the material is a challenging task. The electrochemical performance of a PEMFC, which is sensitive to the physical and chemical nature of the current collectors, is assessed using different materials in this PEMFC test and the polarization curves are plotted. The polarization curve shows the different limiting mechanisms that occurs during the operation [23, 24].

Graphite, Aluminum (Al) and Titanium (Ti) are used as cathode and anode current collector materials during this fuel cell test. The polarization curves for these three cells are compared and illustrated in Fig. 5.The results indicate that the collected current by the collector with Ti are higher than the others; therefore, Ti is recommended. The reason for this is the differences in their properties, specifically conductivity. The property of these three collectors' materials is tabulated in Table 3. The performance of the current collector with a Ti conduction layer is about 6% greater than the one with a graphite layer. Maximum difference occurs at a low voltage of 0.4 (V). Any highly conductive materials can be considered as a candidate for the current collector. The enhancements in cell polarization attributed to the material of the current collectors were featured by a reduction in

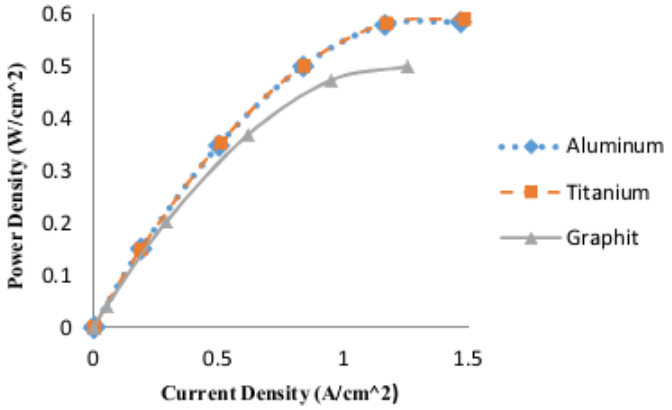

Fig. 5. Comparison of the numerical model prediction for different collectors.

Table 3. Properties of collector material.

Material	Density (g/cm^3)	Thermal conductivity (w/m.k)	Thermal resistivity (Ω.m*10^{-8})	Heat capacity (kj/kg.k)
Al	2.7	237	2.82	0.87
Ti	4.506	21.9	4.2	0.47
graphite	2.25	23.9	6000	0.71

the overall slope of the curve. The slope represents the combined effect of activation over potentials, mass transfer and overall fuel cell resistances [30].

3.2. Effect of CL porosity on power density

Gas must flow through the pores of the CL to the reaction sites, suggesting that porosity could be a significant factor affecting performance. There exists a direct relationship between low porosity and poor performance. The porosity of the CL is determined through the area and mass of the CL.

Three different porosities are assessed in this study. The tested electrodes CL porosities are 0.4, 0.5 and 0.6. The results indicate that the electrode porosity has little effect on performance within the assessed ranges. In this increasing range the electrodes CL is enhanced through reactant and product mass transfer with an effect of less than 1%. Within these ranges, there is no correlation between porosity and performance. This phenomenon is in good agreement with the results obtained by Kong et al. [31], who concluded that pore size distribution within the CL has more significant effect on cell performance than total porosity. Increased porosity results in little advantage when operating at any current density.

3.3. Effect of GDL porosity on power density

GDL porosity varies from 0.7, 0.82 to 0.92. A Comparison of the fuel cell performance at the various mentioned GDL porosities for three collectors at different voltage is presented in Figs. 6, 7 and 8, respectively. As porosity increases, it permits the O_2 within the gas to become closer to the reaction sites in the CL. This increase contributes to electrochemical reaction by providing a higher concentration of O_2 on the catalyst surface. It is the onset of mass transfer limitations, which occurs at higher current densities, which leads to higher limiting currents. Higher porosity implies higher permeability and a less solid region; thus, better flow of reacting gases and lower effective thermal and electrical conductivities are concluded. It is obvious that higher porosity near the interface of CL/GDL is essential for O_2 transfer and H_2O removal. As showed in Figs. 6, 7 and 8, an increase in GDL diffusivity at lower voltage has no significant effect on power density, while in voltages higher than 0.5 (V) it becomes significant. This means that greater porosity of GDL leads to a superior space for the diffusion; however, it also prompts a higher contact resistance in GDL.

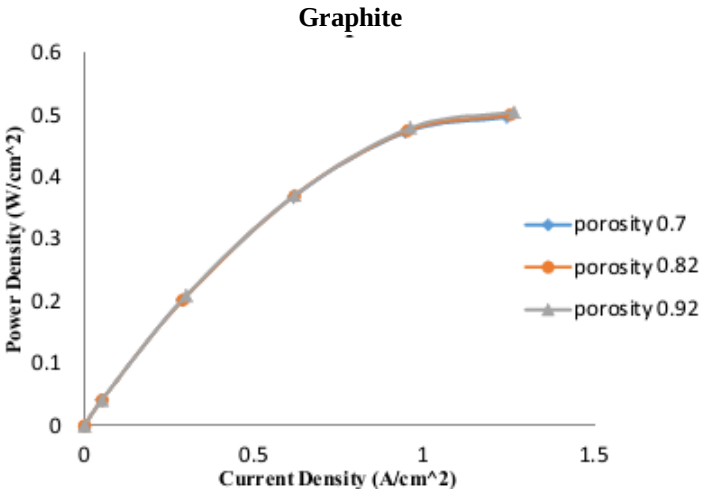

Fig. 6. Comparison of fuel cell performance at different GDL porosity for a graphite collector.

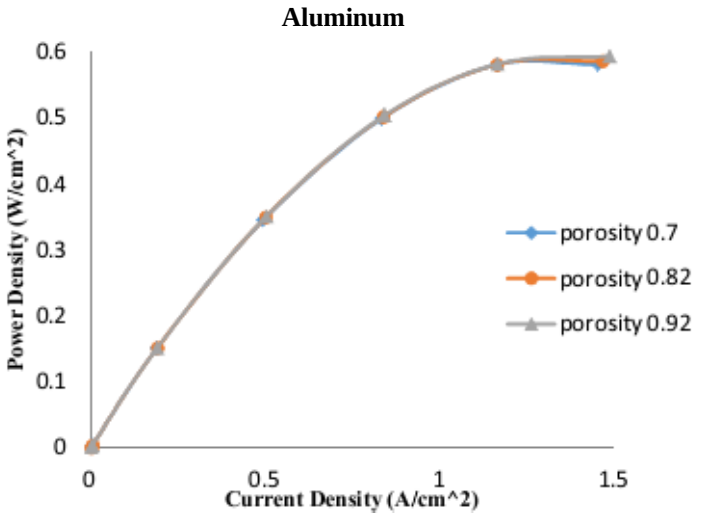

Fig. 7. Comparison of fuel cell performance at different GDL porosity for an aluminum collector.

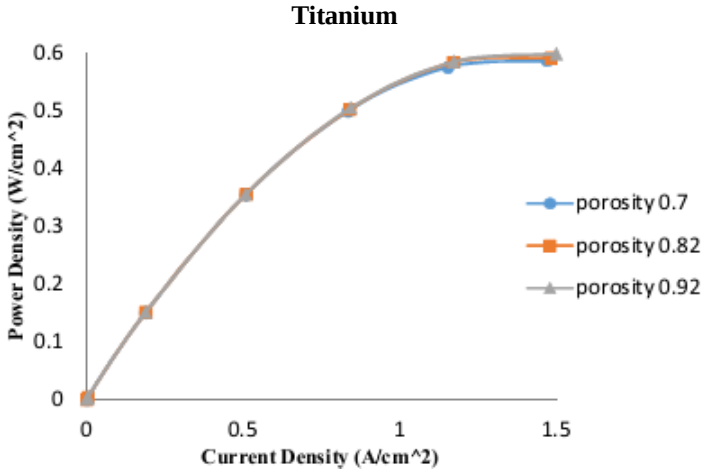

Fig. 8. Comparison of fuel cell performance at different GDL porosity for a titanium collector.

As described the optimum condition is yielded when the voltage is 0.4 (V), the electrode CL porosity is 0.5 (as reference value) and the GDL porosity is 0.92. The 3D concentration distribution of O_2 (cathode) and H_2 (anode) in the PEMFC at optimum condition when the collector is graphite is shown in Figs. 9 and 10, respectively. The concentration distribution of H_2 and O_2 with titanium collectors is shown in Figs. 11 and 12, respectively, and the concentration distribution of H_2 and O_2 with aluminum collector is shown in Figs. 13 and 14, respectively. As observed, their concentration decreases in a gradual manner due to a reduction in the mass fraction of O_2 and H_2 in GDL from inlet to outlet channels. Due to the higher volume flow rates of H_2, H_2 concentrations introduce high values in the electrode region near the gas flow channel as observed at Figs. 9-14.

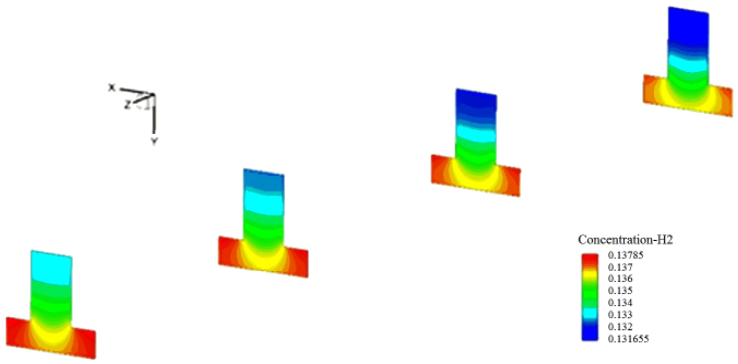

Fig. 9. H_2 concentration distribution in the PEMFC with a graphite collector. Voltage = 0.4 V, electrode porosity= 0.5, gas layer porosity= 0.92.

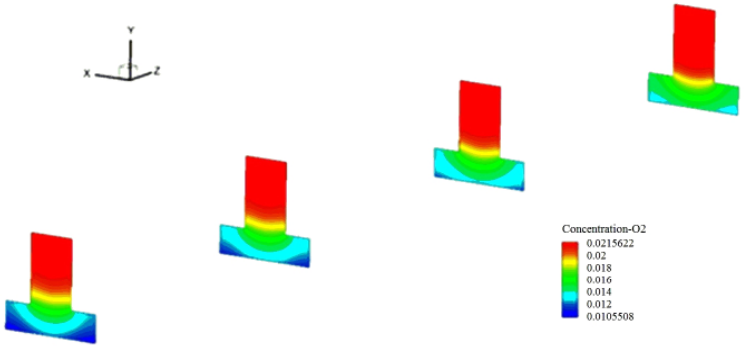

Fig. 10. O_2 concentration distribution in the PEMFC with a graphite collector. Voltage = 0.4 V, electrode porosity= 0.5, gas layer porosity= 0.92.

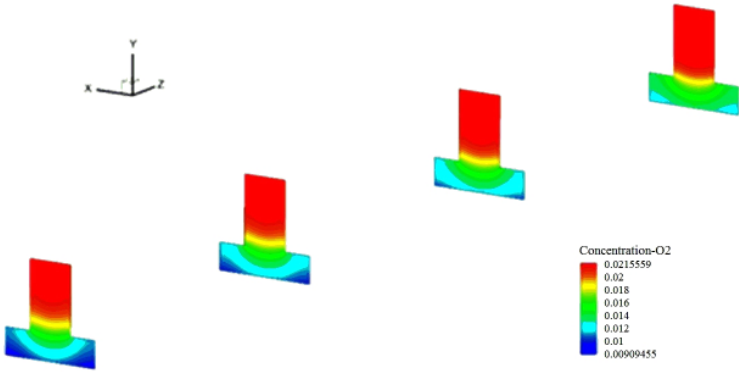

Fig. 11. H_2 concentration distribution in the PEMFC with a titanium collector. Voltage = 0.4 V, electrode porosity= 0.5, gas layer porosity= 0.92.

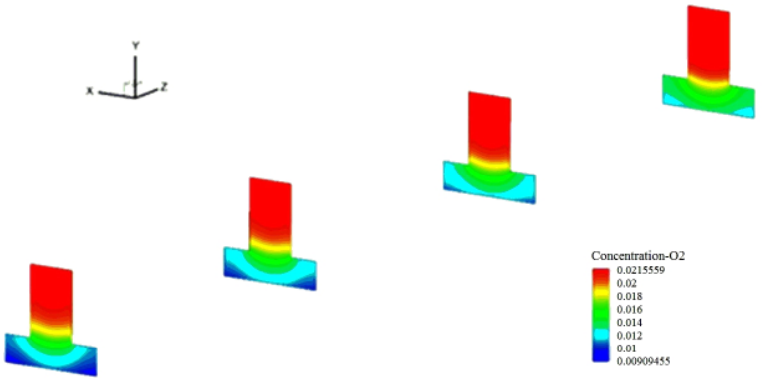

Fig. 12. O_2 concentration distribution in the PEMFC with a titanium collector. Voltage = 0.4 V, electrode porosity= 0.5, gas layer porosity= 0.92.

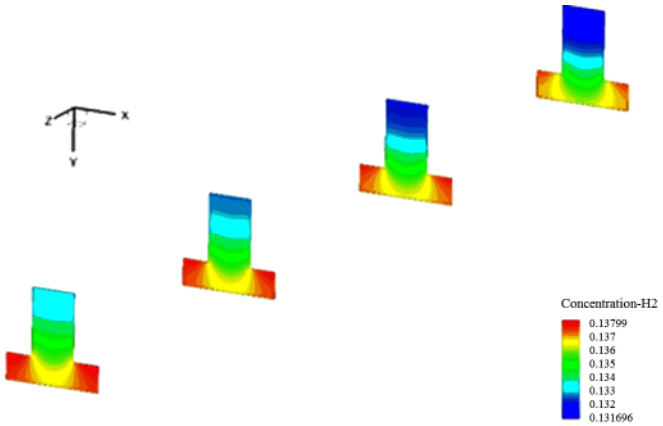

Fig. 13. H_2 concentration distribution in the PEMFC with an aluminum collector. Voltage = 0.4 V, electrode porosity= 0.5, gas layer porosity= 0.92.

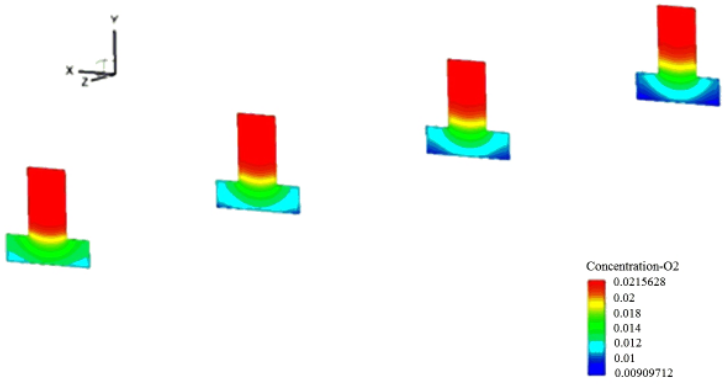

Fig. 14. O_2 concentration distribution in the PEMFC with an aluminum collector. Voltage = 0.4 V, electrode porosity= 0.5, gas layer porosity= 0.92.

4. Conclusions

A single channel PEMFC numerical model with nine zones consisting of two BPs, two gas flow channels, two GDLs, two CLs and a membrane is created and the conclusions thereof obtained from this numerical study are briefed in the following three statements:

1. It is found and verified that titanium enhances the performance of the fuel cell in comparison with graphite and aluminum, therefore a titanium collector is recommended.
2. The total porosity of the electrodes' layers does not have a significant effect on power density.
3. Higher porosity of layer at voltages higher than 0.5

is favorable for gas diffusion, which leads to a better performance.

4. Due to a reduction in the mass fraction of O_2 and H_2 in GDL from inlet to outlet of the channel, their concentration decreases.

5. Higher flow rates of H_2 near the gas flow channel lead to an increase of H_2 concentration in the electrode region.

Nomenclature

A	area, m^2
ac	surface-to-volume ratio, m^2/m^3
a	water activity
C_p	specific heat capacity
C_2	inertial resistance factor, 1/m
D_i	diffusivity of specie i, m^2/s
F	Faraday constant, C/mol
h	enthalpy, J/mol
h_c	free convection heat transfer coefficient, W/m^2K
I	current, A
i	current density, A/m^2
i_0	volumetric reference exchange current density, A/m^3
[i]	molar concentration of specie i, mol/m^3
k	gas permeability, $1/m^2$
K	thermal conductivity
M_w	molecular weight, kg/kmol
T	temperature, K
u, v, w	velocity components, m/s
v_{mag}	velocity magnitude
u_{Pt}	catalyst utilization
V	volume, m^3
V	voltage, V
x, y, z	spatial coordinates, m
y_i	mass fraction of specie i
m_{Pt}	platinum load, kg/m^2
p	pressure, Pa
$p_{c,}$	capillary pressure, Pa
p_{sat}	saturation pressure, Pa
p_v	vapour pressure, Pa
Q_v	volume flow, mlN/min
R	volumetric transfer current, A/m^3
R	universal gas constant, J/K.mol
R_c	contact resistance, U
r	catalyst particle radius, m
r_s	pore blockage exponent
r_w	condensation rate, kg/m^3s
s	liquid water volume fraction
S_f	source of variable f
S_{mass}	mass source term

Greek letters

α	Exchange transfer coefficient
ε	Porosity
δ	Catalytic layer (CL) thickness, m
γ	Concentration exponent
Φ	Generic variable in NeS equation
λ	Water content
φ	Electric potential, V
μ	Dynamic viscosity, Pa.s
θ	Stoichiometric factor
ρ	Density, kg/m^3
σ	Electric conductivity, 1/(U m)
η	Overpotential, V
Γ_f	Diffusivity of variable f
Δx	Mesh spatial resolution, m

Subscripts/superscripts

a	anode
avg	Average
c	cathode
l	liquid phase
m	membrane phase
s	solid phase
t	time, s
ref	Reference

References

[1] J Kasukurthi J., "Optimization of channel geometry in a proton exchange membrane (PEM) fuel cell", University

of Nevada, Las Vegas, 2009.

[2] Kaldellis J. K. and Zafirak D., "Optimum energy storage techniques for the improvement of renewable energy sources-based electricity generation economic efficiency", Energy, 2007, 32: 2295.

[3] Cicconardi S. P, Jannelli E. and Spazzafumo G.,"Hydrogen energy storage: hydrogen and oxygen storage subsystems", Int. J. Hydrog. energy, 1997, 22: 89.

[4] Mehta V. and Cooper J. S, "Review and analysis of PEM fuel cell design and manufacturing", J. Power Sources, 2003, 114: 32.

[5] Wang S. H., Peng J., Lui W. B. and Zhang J. S., "Performance of the gold-plated titanium bipolar plates for the light weight PEM fuel cells", J. Power Sources, 2006, 162: 486.

[6] Kumar A. and Reddy R. G., "PEM fuel cell bipolar plate- material selection, design and integration", Proceeding of the EPD Congress 2002 and Fundamentals of Advanced Materials for Energy Conversion, TMS Annual Meeting, USA, Washington, 2002: 41.

[7] Kumar A. and Reddy R. G., "Materials and design development for bipolar/end plates in fuel cells", Power Sources, 2004, 129: 62.

[8] Roca-Ayats M., Garcia G., Pena M. A. and Martinez-Huerta M. V., "Titanium carbide and carbonitride electrocatalyst supports: modifying Pt–Ti interface properties by electrochemical potential cycling" , J. Mater. Chem. A, 2014, 2: 18786.

[9] Iranzo A., Munoz M., Rosa F. and Pino J., "Numerical model for the performance prediction of a PEM fuel cell. Model results and experimental validation", Int. J. Hydrog. Energy, 2010, 35:11533.

[10] Obaoyopo S. O., Bello-Ochende T. and Meyer J. P., "Modelling and optimization of reactant gas transport in a PEM fuel cell with a transverse pin fin insert in channel flow", Int. J. Hydrog. energy, 2012, 37: 10286.

[11] Wang X. D, Xu J. L. and Lee D. J., "Parameter sensitivity examination for a complete three-dimensional, two-phase, non-isothermal model of polymer electrolyte membrane fuel cell", Int. J. Hydrog. energy, 2012, 37: 15766.

[12] Pasaogullari U. and Wang C. Y., "Two-phase modeling and flooding prediction of polymer electrolyte fuel cells", Electrochem. Soc, 2005, 152: A380.

[13] Djilali N., "Computational modelling of polymer electrolyte membrane (PEM) fuel cells: challenges and opportunities", Energy, 2007, 32: 269.

[14] Taymaz I. and Benli M., "Numerical study of assembly pressure effect on the performance of proton exchange membrane fuel cell", J. Energy, 2010, 35: 2134.

[15] Zhang Z., Wang X., Zhang X. and Jia L., "Optimizing the performance of a single PEM fuel cell. science and technology", J. fuel cell, 2008, 5: 31007.

[16] Ebrahimi I. M. and Eikani M. H., "Three-dimensional modeling of transport phenomena in a planar anode-supported solid oxide fuel cell", Iran. J. Hydrog. Fuel Cell, 2017, 1: 37.

[17] Farzin R., Baheri Islami S. and Hossainpour S., "The effect of increasing the multiplicity of flow fields contact surface on the performance of PEM fuel cell", Iran. J. Hydrog. Fuel Cell, 2017, 1: 69.

[18] Rostami L., Mohamad Goly Nejad P. and Vatani A., "A numerical investigation of serpentine fl ow channel with different bend sizes in polymer electrolyte membrane fuel cells", Energy, 2016, 97: 400.

[19] Vasilyev A., Andrews J., Jackson L. M., Dunnett S. J. and Davies B., "Component-based modelling of PEM fuel cells with bond graphs", Int. J. Hydrogen Energy, 2017, 42: 2940.

[20] Jithin M., Siddharth S., Das M. K. and De A.,

"Simulation of coupled heat and mass transport with reaction in PEM fuel cell cathode using lattice Boltzmann method", Therm. Sci. Eng. Prog., 2017, 4: 85.

[21] Scheuerer M., Heitsch M., Menter F., Egorov Y., Toth I. and Bestion D., "Evaluation of computational fluid dynamic Des, methods for reactor safety analysis (ECORA)", Nucl Eng, 2005, 235: 359.

[22] Wang C. Y., "Fundamental models for fuel cell engineering", Chem. rev., 2004, 104: 4727.

[23] Um S., Wang C.Y. and Chen K. S., "Computational fluid dynamics modeling of proton exchange membrane fuel cells", J. Electrochem soc, 2000, 147: 4485.

[24] Pasaogullari U. and Wang C.Y, "Liquid water transport in gas diffusion layer of polymer electrolyte fuel cells", J. Electrochem soc, 2004, 151: A399.

[25] Springer T.E, Zawodzinski T. A. and Gottesfeld S.,"Polymer electrolyte fuel cell model", J. Electrochem Soc, 1991, 138: 2334.

[26] Tao W. Q, Min C.H, Liu X.L., He Y.L., Yin B.H. and Jiang W.,"Parameter sensitivity examination and discussion of PEM fuel cell simulation model validation: Part I. Current status of modeling research and model development", J. power sources, 2006, 160: 359.

[27] Iranzo A., Monuz M., Lopez E., Pino J. and Rosa F., "Experimental fuel cell performance analysis under different operating conditions and bipolar plate designs", Int. J. Hydrogen Energy, 2010, 35: 11437.

[28]Chervin C., Glass R.S. and Kauzlarich S.M., "Chemical degradation of La 1− x SrxMnO $_3$/Y_2O_3-stabilized ZrO_2 composite cathodes in the presence of current collector pastes", Solid State Ionics, 2005, 176: 17.

[29] Simner S. P., Anderson M. D., Pederson L. R. and Stevenson J. W., "Performance variability of La (Sr) FeO_3 SOFC cathode with Pt, Ag, and Au current collectors", J. Electrochem Soc, 2005, 152: A1851.

[30] Mench M.M., Frontmatter,Wiley Online Library, 2008.

[31] Kong C. S., Kim D .Y., Lee H. K, Shul Y. G. and Lee T. H., "Influence of pore-size distribution of diffusion layer on mass-transport problems of proton exchange membrane fuel cells", J. Power Sources, 2002, 108: 185.